MOLECULAR IMAGING AND BIOLOGY

Published Online: 9 January 2009

Mol Imaging Biol (2009) 11:137–143
DOI: 10.1007/s11307-008-0192-x

BRIEF ARTICLE

Metabolic Changes in the Rodent Brain after Acute Administration of Salvinorin A

Jacob M. Hooker,[1] Vinal Patel,[1] Shiva Kothari,[1] Wynne K. Schiffer[1]

Medical Department, Brookhaven National Laboratory, Upton, NY, 11973, USA

Abstract

Purpose: Salvinorin A (SA) is a potent and highly selective kappa-opioid receptor (KOR) agonist with rapid kinetics and commensurate behavioral effects; however, brain regions associated with these effects have not been determined.

Procedures: Freely moving adult male rats were given SA intraperitoneally during uptake and trapping of the brain metabolic radiotracer, 2-deoxy-2-[F-18]fluoro-D-glucose (FDG), followed by image acquisition in a dedicated animal positron emission tomography (PET) system. Age-matched control animals received vehicle treatment. Animal behavior during FDG uptake was recorded digitally and later analyzed for locomotion. Group differences in regional FDG uptake normalized to whole brain were determined using Statistical Parametric Mapping (SPM) and verified by region of interest (ROI) analysis.

Results: SA-treated animals demonstrated significant increases in FDG uptake compared to controls in several brain regions associated with the distribution of KOR such as the periaqueductal grey, bed nucleus of the stria terminalis and the cerebellar vermis, as well as in the hypothalamus. Significant bilateral activations were also observed in the auditory, sensory, and frontal cortices. Regional decreases in metabolic demand were observed bilaterally in the dorsolateral striatum and hippocampus. Locomotor activity did not differ between SA and vehicle during FDG uptake.

Conclusions: We have provided the first extensive maps of cerebral metabolic activation due to the potent κ-opioid agonist, salvinorin A. A major finding from our small animal PET studies using FDG was that neural circuits affected by SA may not be limited to direct activation or inhibition of kappa-receptor-expressing cells. Instead, salvinorin A may trigger brain circuits that mediate the effects of the drug on cognition, mood, fear and anxiety, and motor output.

Key words: Salvia, Salvinorin A, Kappa opioid, Hallucinogen, Positron emission tomography

Electronic supplementary material The online version of this article (doi:10.1007/s11307-008-0192-x) contains supplementary material, which is available to authorized users.

Significance: Salvinorin A is the major psychoactive compound from *Salvia divinorum* and is a potent kappa-opioid receptor agonist. Owing to its hallucinogenic properties, abuse liability, and medicinal potential as a kappa-agonist there has been a growing effort to characterize its physiological effects in rodents. Our manuscript describes our efforts to further inform how salvinorin A leads to behavioral (and physiological) changes in rodents. We have determined the regional differences (relative to controls) in glucose utilization in the brains of freely behaving rats after acute administration of salvinorin A. Using FDG, we have mapped brain regions that are activated or deactivated as a result of the kappa agonist. We feel there will be an increasing need to systematically understand how affinity, pharmacokinetics, and distribution influence behavior through regional changes in brain activation. Our studies highlight the potential of FDG with small animal PET to accomplish this.

Correspondence to: Jacob M. Hooker; *e-mail:* hooker@bnl.gov; Wynne K. Schiffer; *e-mail:* wynne@bnl.gov

Introduction

Opioid receptor ligands have a rich pharmacology, both beneficial and adverse, often controlling human perceptions of nociception, stress, and danger. Agonists acting at any of the three main classes of opioid receptors (μ, κ, or δ) throughout the central nervous system can cause analgesia and are thus used clinically in pain management [1, 2]. In addition, due to their ability to modulate neurotransmitter release, causing euphoria or dysphoria, opioid ligands have gained attention in the management of mood disorders including depression [3, 4]. Of the three main classes, κ-opioid receptor (KOR) agonists appear to exhibit robust

analgesia with lower abuse potential [5, 8]. Consequently, there have been many research efforts focused on developing selective KOR agonists not only for medicinal uses, but also to study the KOR itself.

One of the most selective KOR agonists known to date comes from nature. Salvinorin A (SA), isolated from *Salvia divinorum*, and many of its semi-synthetic derivatives have proved to be valuable tools to study the KOR system. Several reports have shown the *in vivo* study of SA, a potent and highly selective κ-opioid agonist [9], may provide insight into the role of KORs in mediating both pain and mood [10]. These studies have interrogated the physiological and behavioral effects of SA, which has been increasingly used as a legal hallucinogen [11]. While extremely low doses of SA may be rewarding [12, 13], doses above 0.1 mg/kg (i.p.) caused conditioned place aversion in rodents and decreased extracellular dopamine in the striatum, consistent with the effects of other κ-agonists [14, 15]. In addition, acute administration of SA increased the occurrence of immobility in the forced swim test and the threshold for intracranial self-stimulation [16, 17]. The antinociceptive and sedative effects of SA were demonstrated in mice by observing latency in the radiant heat tail flick assay [18, 19], decreased locomotion [14], impaired climbing behavior [20], and abdominal constriction test [21].

The pharmacological effects of SA appear to be highly specific to the κ-opioid receptor as proposed by *in vitro* studies [9]. This has been supported by successful blockade of physiological and behavioral effects *in vivo* with KOR antagonists, the use of KOR knockout mice [19], and KOR discriminatory tests [22]. Of course, binding at the initial site of action (i.e., the KOR) leads to many physiological changes in the brain, notable for example in decreases in striatal dopamine. The downstream effects of SA on brain function (i.e., changes secondary to neuron firing) are largely unknown. With the goal of associating brain regions and perhaps neuronal circuits involved in SA-mediated effects, we have examined regional changes in 2-deoxy-2-[F-18]-fluoro-D-glucose (FDG) uptake in the rat brain. Using this technique, the current study provides the first extensive maps of cerebral metabolic activation together with behavior in response to SA in freely moving adult rats.

Materials and Methods

Animals

All animal procedures were performed in accordance with the National Institutes of Health Guide for the Care and Use of Laboratory Animals and were approved by the BNL Institutional Animal Care and Use Committee. Twenty male Sprague–Dawley rats (7–8 weeks old, Taconic Farms) were used for this study. Paired animals were housed in cages and were maintained on a 12:12 light/dark cycle with free access to food and water. Three days prior to imaging, animals were individually housed. A group of ten animals served as the control (vehicle only) and the remaining ten animals were given salvinorin A. All 20 animals received FDG. Data collected from 19 of the 20 animals was used (as one animal died as a result of anesthesia).

Materials

Salvinorin A was extracted and purified from dried leaves of *Salvia divinorum* (Bouncing Bear Botanicals) as previously described [23]. Salvinorin A used for animal studies was recrystallized from absolute ethanol until its purity was greater that 99.5% as determined by ^{1}H NMR and C18 HPLC (monitored at 214 nm). Anesthesia was induced using a mixture of ketamine and xylazine (both from Fort Dodge, Fort Dodge, IA, USA) as intraperitoneal injections of 50 mg/kg ketamine with 5 mg/kg xylazine. FDG was prepared at Brookhaven National Laboratory from [^{18}F]fluoride using a Bioscan® synthesis unit.

Protocol

On the day before the study, animals were weighed (285±14 g), placed in a clean (home) cage and transported to the positron emission tomography (PET) facility. Animals arrived at the facility approximately 16 h prior to scanning to habituate to their environment and were deprived of access to food 6 h prior to scanning to stabilize plasma glucose, as well as to prevent interference with anesthesia, which was administered after the uptake period but prior to scanning. The experimental timeline for each subject is outlined in Fig. 1. Salvinorin A or vehicle (2.0 mg/kg in DMSO) and FDG (1.04±0.14 mCi, 0.5 mL in saline) were administered intraperitoneally.

Locomotion

Animal behavior was recorded digitally during the FDG uptake period (i.e., from 12 min post injection of SA to 60 min post

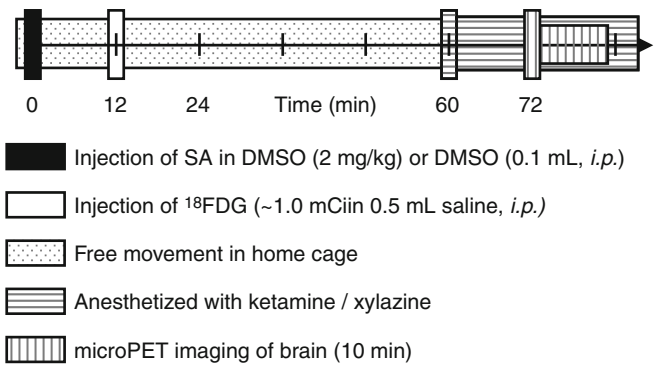

Fig. 1. Imaging protocol timeline for determination of metabolic changes resulting from salvinorin A.

injection). The video data were analyzed using TopScan® "Top-view Animal Behavior Analyzing System" (Clever Sys., Inc.). Animal tracking data (locomotion) were binned in three 12-min intervals. Data for the first 5 min (i.e., 12–17 min post-SA injection) were also binned for separate comparison. Video data from nine of the animals (five DMSO control animals and four SA-injected animals) were not used due to image file corruption. Locomotion (i.e., distance traveled per binned time) for the two groups (DMSO control, $n=5$; SA, $n=6$) was compared by means of a two tailed T-test.

Image Acquisition

Each FDG-PET scan included subtraction of random coincidences collected in a delayed time window. Three dimensional (3D) sinograms were converted into 2D sinograms before image reconstruction. This was done with the process of Fourier rebinning. After Fourier rebinning, images were reconstructed by 2D-filtered back projection using a ramp filter with cutoff at one-half the Nyquist criteria (maximum sampling frequency). Data were corrected for photon scatter using the method of tailfitting of the projections [24]. At the time of these studies, the measured attenuation correction method available for this system used a ^{68}Ge point source and contributed a degree of noise to the transmission scans [24]. Therefore, attenuation correction was not applied. In general, attenuation correction factors are constant over time and should similarly influence all data. Scatter-corrected sinograms were reconstructed using an iterative maximum likelihood expectation maximization (MLEM) algorithm, which with the 20 iterations employed here yields an image resolution of ~1.5 mm FWHM (Full Width at Half Maximum) at the center of the field of view. The image pixel size in MLEM reconstructed images was 0.4 mm trans-axially with a 1.21 mm slice thickness. Regions of Interest (ROIs) were drawn on MLEM reconstructed images for estimation of regional FDG uptake.

Post Acquisition Processing

To compare data across subjects, each PET scan was transformed into the same coordinate system using standard analysis methodology developed for human functional imaging experiments. A crucial aspect of whole brain inter-subject comparisons is to obtain an accurate fit of the brains from all subjects into the same coordinate space, such that each brain structure resides in the same location for all subjects. A multi-stage process was used to create a study-specific PET template and then spatially preprocess and spatially normalize each PET scan to the FDG-PET template. Creation of the template has been described elsewhere [25]. Regions of interest were identified in Paxinos and Watson stereotaxic space [26], and an ROI template was developed and implemented using Pixelwise Modeling software (PMOD; http://www.pmod.com)[27].

To facilitate inter-subject comparisons, each image was given the same mean value by applying a global scale factor to each scan. Global scale factors were determined by adjusting the mean based on a whole brain ROI that excluded regions outside the brain.

Spatial Preprocessing

PET images from each subject were initially matched to the template space manually, which included a shift, a rotation, a zoom, and a perspective transformation in each of the three dimensions (x, y, and z) to match the location and bounding box of the template brain [28]. This transformation matched the size, location, and orientation of each individual brain to that of the PET template. These images were coregistered to each other and to the non-skull stripped PET template using the normalized mutual information algorithm implemented with the SPM2 software package. Coregistered images were then skull stripped and smoothed with a 4-mm FWHM Gaussian filter. The masked or skull stripped images were then coregistered and normalized to the FDG template using the same parameters described for creating the template [25]. Each step of the spatial pre-processing was manually verified and final images were investigated in detail.

Statistical Design and Analysis in SPM

Next, to ensure that only voxels mapping cerebral tissue were included in the analysis, voxels for each brain failing to reach a specified threshold were masked out to eliminate the background and ventricular spaces. We set the default threshold to 80% of the mean voxel value inside the brain. To examine regional brain differences between control animals and those given SA, an image contrast analysis was performed where the difference between the two groups of scans was calculated and represented in three-dimensional space by a map of the t-statistic. SPM t-maps represent spatially extended statistical results, which were used to identify regionally specific differences in the imaging data. Small volume correction was applied post hoc in SPM to determine the significance of region by sampling from a sphere of 1 mm around the most significant voxel in each cluster.

Results and Discussion

Previously, we demonstrated that [^{11}C]-salvinorin A, given intravenously in non-human primates, rapidly enters the brain, distributes in a high concentration to the cerebellum and throughout the cortex, but persists in the brain for only minutes [29]. Indeed, we found that a similar distribution occurred in the rat brain with even faster kinetics such that binding was difficult to discriminate from blood flow (time to peak, 20 s; half life from peak, 180 s). Clearly, the pharmacological duration of action of SA and its unique abuse liability as a KOR agonist directly correlate with its kinetics, but so far the kinetics and distribution provide limited insight into the behavioral effects seen in rodents.

To examine the effects of SA on regional brain function, we investigated regional brain metabolic changes in rodents given an acute dose of SA (2.0 mg/kg i.p. in DMSO). Control animals were given vehicle injections of DMSO using an identical protocol. By imaging the rodent brain with small animal positron emission tomography (mPET) after

administration of SA and FDG, regional drug-dependent differences were determined. Patterns of change in FDG uptake associated with drug administration give a measure of the downstream effects of drug action. Regional patterns of activation and deactivation in response to an acute drug challenge can be used to identify a metabolic 'signature' comprised of relevant regions of the brain for different compounds within the same chemical class, or different chemical classes. Many SA behavioral paradigms in the literature have pointed to depression, antinociception, and decreased locomotion as prominent effects of SA administration. We anticipate that combining these behavioral observations with information about discrete metabolic changes in the rat brain when exposed to SA (reported herein), will offer a more complete understanding of the pharmacological properties of this potent and selective KOR agonist.

Our experimental design was guided by behavioral and physiological data in the literature [14, 16, 17]. In rodents, SA (*i.p.*) quite consistently reached its maximum effect between 20 and 40 min, as measured through behavioral challenge or dopamine change measure via microdialysis. Thus, we designed our experimental protocol to allow for

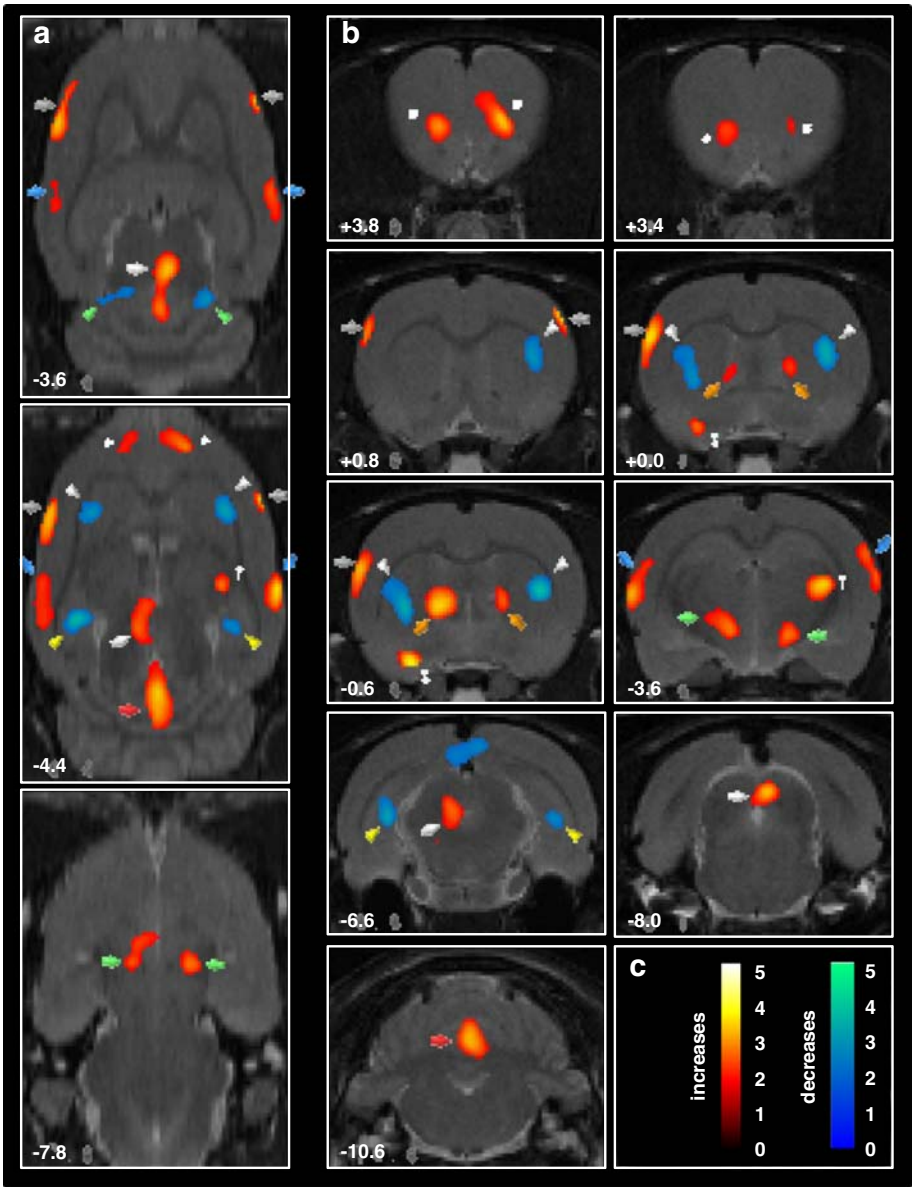

Fig. 2. Regional differences in functional brain activity in rats given SA ($n=10$) compared to vehicle-treated controls ($n=9$). Depicted is a selection of representative transaxial (a) and coronal (b) slices. Colored overlays show statistically significant positive (red scale) and negative (blue scale) differences at a voxel level ($P<0.05$ with an extent threshold of 100 contiguous voxels), with the *t*-statistic indicated in (c). In (a), the distance below bregma is indicated in the lower left corner while in (b), the distance anterior (positive numbers) or posterior (negative numbers) from bregma is given in the lower left corner of the slice. Marked regions and their significance are listed in Table 1.

maximal FDG uptake during this period, Fig. 1. After administering SA (2.0 mg/kg i.p.) or vehicle only (0.1 mL DMSO), each animal was returned to its home-cage for 12 min. Following this, FDG (nominally 1.0 mCi, i.p.) was given. FDG administered in this manner reaches a maximum concentration in the brain in 10–15 min, which corresponds to 22–27 min post administration of SA [27]. Thus, using this timeline, the peak of FDG uptake into the brain was timed to coincide with of that of SA.

Animals were allowed to behave freely until 1 h post-SA administration at which time they were anesthetized with ketamine/xylazine. Each animal's locomotion was recorded during the FDG uptake period (i.e., 12–60 min post-SA injection). Analysis of locomotion data indicated no statistically significant difference between the two groups of animals (all analyzed time bins, $P>0.3$). While a single acute dose did not have an effect on locomotion, in subsequent experiments we observed locomotion changes after multiple acute doses (see electronic supplementary material).

After imaging and data processing (see details in methods), groups of images (SA, $n=9$; vehicle, $n=10$) were compared using statistical parametric mapping (SPM). Using a statistical tolerance of $P<0.05$, t-map images were generated and superimposed on a MRI template of the rat [28], all in stereotaxic space. Representative two-dimensional images from this three-dimensional data set are shown in Fig. 2.

The data were interrogated at the cluster level and assigned to a structural region. The percent change (either increase or decrease) in FDG uptake for the group of SA images relative to DMSO controls was determined using a spherical region of interest of 2.5 mm diameter surrounding the voxel of greatest intensity (i.e., highest statistical significance) within each cluster. This ensured minimal overlap in cluster analysis. The results of SPM and subsequent analysis are summarized in Table 1.

All of the data showed striking symmetric bilaterally suggesting a high degree of fidelity. The absolute magnitude of change may be masked by using a whole brain normalization, which eliminates differences in absolute FDG uptake, but nonetheless the regional interrogation and results can be used for hypothesis driven behavioral research on SA and its derivatives in the future.

As might be expected, several regions with high KOR density did indeed show increased FDG uptake. Of particular note, the periaqueductal gray (PAG), showed increased metabolic activity (Fig. 2a, white arrow). This cerebral duct within the midbrain has a very high density of KOR and has been repeatedly correlated with modulation of pain, as well as in defensive behavior and fear conditioning [30]. Activation of KORs in the dorsal PAG has also been linked with defensive behavior in rats tested in the elevated plus maze [31]. We also observed significant bilateral activation of the bed nucleus of the stria terminalis (BNST;

Table 1. Summary of cluster- and voxel-level statistics determined with SPM

Contrast	Cluster level	Voxel level			Coordinates[a]			Region	% Change	Symbol in Fig. 2
	p_{SVC}	T	($Z_{=}$)	p_{uncorr}	x,y,z {mm}					
Increases	0.049	3.37	2.91	0.002	−0.2	−10	−4.2	CB-vermis	7.9	Red arrow
	0.043	2.57	2.33	0.01	−0.8	−6.4	−4.6	PAG	6.5	White arrow
	0.045	4.96	3.85	0	7	−4.6	−5.2	R AuTeA	6.7	Blue arrow
	0.042	3.2	2.79	0.003	−6.8	−4	−5.6	L AuTeA	7.3	Blue arrow
	0.044	4.06	3.35	0	−2	−1.2	−5.8	L Septum/BNST	6.9	Orange arrow
	0.043	3.2	2.79	0.003	4	−1	−5.8	R Septum/BNST	5.5	Orange arrow
	0.037	4.16	3.41	0	−3	−1.2	−9.4	L VP	9.9	Double dagger
	0.036	2.72	2.45	0.007	−1.4	−3.8	−7.2	L PH	4.3	Green arrow
	0.045	3.39	2.92	0.002	3.8	−3.8	−5	R LH	4.5	Green arrow
	0.077	2.83	2.53	0.006	−1.6	3.8	−5.2	L OFC	5	Astericks
	0.081	3.23	2.82	0.002	2	3.8	−4.8	R OFC	5.4	Astericks
	0.076	3.48	2.98	0.001	−5.8	0.2	−4	L S1	6.2	Grey arrow
	0.128	3.32	2.88	0.002	5.6	1.2	−3.2	R S1	5.4	Grey arrow
	0.083	3.29	2.85	0.002	3.8	−3.8	−5	R LG	7.5	Dagger
Decreases	0.043	4.73	3.73	0	4	−1.2	−5.2	R CPu	−5.8	White arrowhead
	0.043	3.67	3.1	0.001	−3.4	−0.8	−6.4	L CPu	−6.8	White arrowhead
	0.037	3.77	3.17	0.001	2.2	−5.6	−6.4	R Brainstem	−6.3	Not shown
	0.037	3.53	3.01	0.001	−2.8	−6.4	−5	L Brainstem	−4.4	Not shown
	0.049	3.32	2.87	0.002	−2.2	−9.6	−2.8	L SC	−10	Green arrowhead
	0.042	3.52	3.01	0.001	2.6	−9.2	−2.2	R SC	−7.8	Green arrowhead
	0.043	2.72	2.44	0.007	−4.8	−7.2	−6.4	L Hippocampus	−5.9	Yellow arrowhead
	0.044	3.95	3.28	0.001	−2.2	−12.8	−4.2	R Hippocampus	−6.3	Yellow arrowhead

Significance is shown for clusters exceeding 100 contiguous voxels after correction for Small Volumes (SVC), performed for each region using a 1-mm diameter sphere around the pixel of greatest change. Coordinates are given in Paxinos and Watson stereotaxic space [26], where *R* indicates the right hemisphere and *L* indicates the Left hemisphere: *CB* (cerebellum), *PAG* (periaqueductal grey), *AuTeA* (Auditory Temporal Association Area, *BNST* (Bed Nucleus of the Stria Terminalis), *VP* (Ventral Pallidum), *PH* (Posterior Hypothalamus), *LH* (Lateral Hypothalamus), *OFC* (Orbitofrontal cortex), *S1* (primary sensory cortex), *LG* (Lateral Geniculate nucleus), *CPu* (Caudate Putamen), *SC* (Superior Colliculus).

[a]Coordinates are given for the voxel with the greatest significance within a cluster.

Fig. 2b, orange arrows), a region with high density of KOR (Mansour et al. 1996). In addition, the vermis of the cerebellum was highly activated. This region has recently been ascribed the function of proprioception in animals although it is unclear whether activation would impair or enhance spatial awareness [32].

Regional differences in FDG uptake were not limited to brain regions associated with a high density of KOR. Significant bilateral activations were also observed in regions which have little or no KORs, such as the hypothalamus, auditory, sensory and frontal cortices (Fig. 2). Relative increases in FDG uptake were also observed unilaterally in the left ventral pallidum and right lateral geniculate nuclei. These regional differences may reflect neuronal activity downstream from the changes in neural activity at sites with high KOR density, as well as the subsequent recruitment of additional brain regions.

Bilateral metabolic decreases were observed in the caudate putamen, superior colliculus, hippocampus, and medial brainstem (Fig. 2, blue regions). These results show that the metabolic response to SA goes well beyond the immediate KOR effects and involve a larger activation of neuronal circuits projecting from the primary KOR sites to functionally and anatomically related regions of the brain. For instance, decreases in metabolism may result from activation of inhibitory neurons projecting to these regions. With only a map of relative local glucose utilization, distinguishing between changes resulting from local cellular interactions and those that are inter-neuron mediated is not possible. For a review on the role of inhibitory inter-neurons on the brain's energy consumptions, see Buzsáki et al. [33].

Here, we show localized changes in brain activity resulting from an acute challenge of SA that are specific and extend beyond its initial site of action. Although we can only speculate at this point on the relationship of activation or deactivation of particular brain regions to behavior, we feel these data may provide a basis for interrogating the effects of SA in rodents in the future. Identification of brain regions demonstrating changes in neural activation in response to SA may inform the design of future analogs of SA and may provide an experimental platform for simultaneous testing of the pharmacodynamic and behavioral effects of these new compounds in the same animal. For example, structural manipulations of SA, *in vitro* structure–activity relationships, and an understanding of molecular interactions can lead to more potent and longer-lasting drugs [34–37]. The impact of these developments, both physiologically and behaviorally, can be marked [38]. We feel there will be an increasing need to systematically understand how affinity, pharmacokinetics, and distribution influence behavior through regional changes in brain activation. Our studies highlight the potential of FDG with small animal PET to accomplish this.

Finally, it is worth noting that the route of SA administration (i.p.) may have a prevailing impact on pharmacodynamics and behavior in animals as noted in the human experience [39]. We are currently investigating how the route of administration (and therefore SA pharmacokinetics) effects brain glucose utilization as well as probing the effects of other SA derivatives that exhibit longer last effects.

Conclusion

By investigating the effects of salvinorin A on local glucose utilization in the rat brain, we have provided the first extensive maps of cerebral metabolic activation due to this potent κ-opioid agonist. A major finding from our small animal PET studies using FDG were that neural circuits affected by SA could be observed in the absence of any observable behavioral effects. The neural circuits that we have identified through this study include regions known to have high κ-opioid receptor density as well as in functionally related brain regions with known anatomical connections. This would suggest that important data lie in our examination of distributed changes in brain metabolism in various relevant regions of the brain. Future studies combining behavioral paradigms with cerebral metabolic mapping are aimed at further elucidating the effects of SA in the rodent brain. Moreover, analogous studies with new and more potent SA derivatives may point to potential KOR therapeutic agents and will increase our understanding of their effects on pain and depression.

Acknowledgments. This work was carried out at Brookhaven National Laboratory under contract DE-AC02-98CH10886 with the U.S. Department of Energy and supported by its Office of Biological and Environmental Research. J.M.H. was supported by an NIH Postdoctoral Fellowship (1F32EB008320-01) and through the Goldhaber Distinguished Fellowship program at BNL. The authors are grateful to Dr. Stephen Dewey, David Alexoff, and Dr. Martine Mirrione for helpful discussions and insights.

References

1. Ossipov MH, Lai J, King T, Vanderah TW, Malan TP Jr, Hruby VJ, Porreca F (2004) Antinociceptive and nociceptive actions of opioids. J Neurobiol 61:126–148
2. Snyder SH, Pasternak GW (2003) Historical review: opioid receptors. Trends Pharmacol Sci 24:198–205
3. Mague SD, Pliakas AM, Todtenkopf MS, Tomasiewicz HC, Zhang Y, Stevens WC Jr, Jones RM, Portoghese PS, Carlezon WA Jr (2003) Antidepressant-like effects of kappa-opioid receptor antagonists in the forced swim test in rats. J Pharmacol Exp Ther 305:323–330
4. Jutkiewicz EM (2006) The antidepressant-like effects of delta-opioid receptor agonists. Mol Interv 6:162–169
5. Pan ZZ (1998) mu-Opposing actions of the kappa-opioid receptor. Trends Pharmacol Sci 19:94–98
6. Hunter JC, Leighton GE, Meecham KG, Boyle SJ, Horwell DC, Rees DC, Hughes J (1990) CI-977, a novel and selective agonist for the kappa-opioid receptor. Br J Pharmacol 101:183–189
7. Tao YM, Li QL, Zhang CF, Xu XJ, Chen J, Ju YW, Chi ZQ, Long YQ, Liu JG (2008) LPK-26, a novel kappa-opioid receptor agonist with potent antinociceptive effects and low dependence potential. Eur J Pharmacol 584:306–311
8. Millan MJ (1990) Kappa-opioid receptors and analgesia. Trends Pharmacol Sci 11:70–76
9. Roth BL, Baner K, Westkaemper R, Siebert D, Rice KC, Steinberg S, Ernsberger P, Rothman RB (2002) Salvinorin A: a potent naturally

occurring nonnitrogenous kappa opioid selective agonist. Proc Natl Acad Sci U S A 99:11934–11939
10. Vortherms TA, Roth BL (2006) Salvinorin A: from natural product to human therapeutics. Mol Interv 6:257–265
11. Babu KM, McCurdy CR, Boyer EW (2008) Opioid receptors and legal highs: Salvia divinorum and Kratom. Clin Toxicol (Phila) 46:146–152
12. Braida D, Limonta V, Capurro V, Fadda P, Rubino T, Mascia P, Zani A, Gori E, Fratta W, Parolaro D, Sala M (2008) Involvement of kappa-opioid and endocannabinoid system on Salvinorin A-induced reward. Biol Psychiatry 63:286–292
13. Braida D, Limonta V, Pegorini S, Zani A, Guerini-Rocco C, Gori E, Sala M (2007) Hallucinatory and rewarding effect of salvinorin A in zebrafish: kappa-opioid and CB1-cannabinoid receptor involvement. Psychopharmacology 190:441–448
14. Zhang Y, Butelman ER, Schlussman SD, Ho A, Kreek MJ (2005) Effects of the plant-derived hallucinogen salvinorin A on basal dopamine levels in the caudate putamen and in a conditioned place aversion assay in mice: agonist actions at kappa opioid receptors. Psychopharmacology (Berl) 179:551–558
15. Gehrke BJ, Chefer VI, Shippenberg TS (2008) Effects of acute and repeated administration of salvinorin A on dopamine function in the rat dorsal striatum. Psychopharmacology 197:509–517
16. Carlezon WA (2006) Neurobiological effects of salvinorin A in rodents: implications for the study and treatment of depressive disorders. Neuropsychopharmacology 31:S40–S41
17. Carlezon WA Jr., Beguin C, DiNieri JA, Baumann MH, Richards MR, Todtenkopf MS, Rothman RB, Ma Z, Lee DY, Cohen BM (2006) Depressive-like effects of the kappa-opioid receptor agonist salvinorin A on behavior and neurochemistry in rats. J Pharmacol Exp Ther 316:440–447
18. John TF, French LG, Erlichman JS (2006) The antinociceptive effect of salvinorin A in mice. Eur J Pharmacol 545:129–133
19. Ansonoff MA, Zhang JW, Czyzyk T, Rothman RB, Stewart J, Xu H, Zjwiony J, Siebert DJ, Yang F, Roth BL, Pintar JE (2006) Antinociceptive and hypothermic effects of salvinorin A are abolished in a novel strain of kappa-opioid receptor-1 knockout mice. J Pharmacol Exp Ther 318:641–648
20. Fantegrossi WE, Kugle KM, Valdes LJ 3rd, Koreeda M, Woods JH (2005) Kappa-opioid receptor-mediated effects of the plant-derived hallucinogen, salvinorin A, on inverted screen performance in the mouse. Behav Pharmacol 16:627–633
21. Wang Y, Tang K, Inan S, Siebert D, Holzgrabe U, Lee DY, Huang P, Li JG, Cowan A, Liu-Chen LY (2005) Comparison of pharmacological activities of three distinct kappa ligands (Salvinorin A, TRK-820 and 3FLB) on kappa opioid receptors *in vitro* and their antipruritic and antinociceptive activities *in vivo*. J Pharmacol Exp Ther 312:220–230
22. Butelman ER, Harris TJ, Kreek MJ (2004) The plant-derived hallucinogen, salvinorin A, produces kappa-opioid agonist-like discriminative effects in rhesus monkeys. Psychopharmacology 172:220–224
23. Lee DY, Karnati VV, He M, Liu-Chen LY, Kondaveti L, Ma Z, Wang Y, Chen Y, Beguin C, Carlezon WA Jr., Cohen B (2005) Synthesis and *in vitro* pharmacological studies of new C(2) modified salvinorin A analogues. Bioorg Med Chem Lett 15:3744–3747
24. Alexoff DL, Vaska P, Marsteller D, Gerasimov T, Li J, Logan J, Fowler JS, Taintor NB, Thanos PK, Volkow ND (2003) Reproducibility of 11C-raclopride binding in the rat brain measured with the microPET R4: effects of scatter correction and tracer specific activity. J Nucl Med 44:815–822
25. Frumberg DB, Fernando MS, Lee DE, Biegon A, Schiffer WK (2007) Metabolic and behavioral deficits following a routine surgical procedure in rats. Brain Res 1144:209–218
26. Paxinos G, Watson C (1986) The rat brain in stereotaxic coordinates, 2nd edn. Academic, New York
27. Schiffer WK, Mirrione MM, Dewey SL (2007) Optimizing experimental protocols for quantitative behavioral imaging with 18F-FDG in rodents. J Nucl Med 48:277–287
28. Schweinhardt P, Fransson P, Olson L, Spenger C, Andersson JL (2003) A template for spatial normalisation of MR images of the rat brain. J Neurosci Methods 129:105–113
29. Hooker JM, Xu Y, Schiffer W, Shea C, Carter P, Fowler JS (2008) Pharmacokinetics of the potent hallucinogen, salvinorin A in primates parallels the rapid onset, short duration of effects in humans. Neuroimage 41:1044–1050
30. Holschneider DP, Yang J, Sadler TR, Nguyen PT, Givrad TK, Maarek JM (2006) Mapping cerebral blood flow changes during auditory-cued conditioned fear in the nontethered, nonrestrained rat. Neuroimage 29:1344–1358
31. Nobre MJ, Ribeiro dos Santos N, Aguiar MS, Brandao ML (2000) Blockade of mu- and activation of kappa-opioid receptors in the dorsal periaqueductal gray matter produce defensive behavior in rats tested in the elevated plus-maze. Eur J Pharmacol 404:145–151
32. Yakusheva TA, Shaikh AG, Green AM, Blazquez PM, Dickman JD, Angelaki DE (2007) Purkinje cells in posterior cerebellar vermis encode motion in an inertial reference frame. Neuron 54:973–985
33. Buzsaki G, Kaila K, Raichle M (2007) Inhibition and brain work. Neuron 56:771–783
34. Beguin C, Richards MR, Li JG, Wang Y, Xu W, Liu-Chen LY, Carlezon WA Jr, Cohen BM (2006) Synthesis and *in vitro* evaluation of salvinorin A analogues: effect of configuration at C(2) and substitution at C(18). Bioorg Med Chem Lett 16:4679–4685
35. Lee DYW, Ma ZZ, Liu-Chen LY, Wang YL, Chen Y, Carlezon WA, Cohen B (2005) New neoclerodane diterpenoids isolated from the leaves of Salvia divinorum and their binding affinities for human kappa opioid receptors. Bioorg Med Chem 13:5635–5639
36. Holden KG, Tidgewell K, Marquam A, Rothman RB, Navarro H, Prisinzano TE (2007) Synthetic studies of neoclerodane diterpenes from *Salvia divinorum*: Exploration of the 1-position. Bioorg Med Chem Lett 17:6111–6115
37. Munro TA, Duncan KK, Xu W, Wang Y, Liu-Chen LY, Carlezon WA Jr., Cohen BM, Beguin C (2008) Standard protecting groups create potent and selective kappa opioids: salvinorin B alkoxymethyl ethers. Bioorg Med Chem 16:1279–1286
38. Wang Y, Chen Y, Xu W, Lee DY, Ma Z, Rawls SM, Cowan A, Liu-Chen LY (2008) 2-Methoxymethyl-salvinorin B is a potent kappa opioid receptor agonist with longer lasting action *in vivo* than salvinorin A. J Pharmacol Exp Ther 324:1073–1083
39. Siebert DJ (1994) *Salvia divinorum* and salvinorin A: new pharmacologic findings. J Ethnopharmacol 43:53–56